SECED 2015 Conference: Earthquake Risk and Engineering towards a Resilient World
9-10 July 2015, Cambridge UK

PROBABILISTIC ASSESSMENT OF ROCKING RESPONSE FOR SIMPLY-SUPPORTED RIGID BLOCKS

Elia VOYAGAKI[1] and Dimitrios VAMVATSIKOS[2]

Abstract: A probabilistic assessment of the rocking and overturning response of a simply-supported rigid block on a horizontal plane is reported. A two-dimensional rectangular block resting on a rough, horizontal, tensionless and cohesionless rigid base at ground surface is considered, subjected to far field horizontal earthquake excitations. The roughness of the interface is assumed to be sufficiently large to prevent sliding, while the flexibility of the block is neglected. Rocking response curves are calculated for increasing ground motion intensity (or, equivalently, decreasing uplift strength) via Incremental Dynamic Analysis (IDA), and results are summarised in the form of 16%, 50% and 84% fractile IDA curves. By employing non-linear regression analysis, simple expressions are developed for each fractile of peak response to offer a complete probabilistic characterisation of rocking behaviour. Generalised overturning criteria are proposed covering a wide set of excitations and block parameters.

Introduction

The rocking response of un-deformable free standing blocks to earthquake ground shaking has been a subject of intense investigations for many years. Despite its apparent simplicity, the problem is difficult to treat analytically, as determining the response can be challenging even for the simplest waveforms due to inherent nonlinearities and other mathematical complexities. Only a handful of cases have been solved completely, mostly for pulses of half-cycle duration (Housner 1964, Shi et al. 1996, Voyagaki et al. 2013), whereas for full-cycle pulses exact analytical solutions are even fewer (Dimitrakopoulos and DeJong 2012, Voyagaki et al. 2014). Extending the overturning criteria to actual ground motions is impossible, as the overturning or survival of a block depends on the details of excitation. In light of this need, a pertinent probabilistic treatment of block response appears desirable.

In the context of two-dimensional rigid-body dynamics, we investigate the numerical problem with the results post-processed in a probabilistic manner, to provide simple response criteria applicable to a wide range of far-field earthquake motions. The methodology of Incremental Dynamic Analysis (Vamvatsikos and Cornell 2002, 2004) is employed to this end. Non-linear regression analyses provided the means for developing simple parametric equations that offer a complete probabilistic characterisation of rocking response for use in Performance-Based Earthquake Engineering (PBEE).

Problem definition

The problem under investigation concerns rocking of a rigid block resting on a rough horizontal rigid plane, subjected to a suite of earthquake motions acting parallel to the plane (Fig.1a). The block is of rectangular shape having mass m, dimensions $(2\mathrm{x}b)$ by $(2\mathrm{x}h)$ – leading to a radial distance from the center of rotation to the center of gravity $R=(b^2+h^2)^{1/2}$ and a dimensionless slenderness angle $\alpha=\tan^{-1}(b/h)$. The friction coefficient at the interface between block and base is assumed to be sufficiently large to prevent sliding, while the flexibility of the block and aerodynamic effects are neglected. The restoring force is shown in Fig.1b.

[1] Research Associate, University of Bristol, UK and J.B. ATE, Heraklion, Greece, e.voyagaki@bristol.ac.uk
[2] Lecturer, National Technical University of Athens, Athens, Greece, divamva@central.ntua.gr

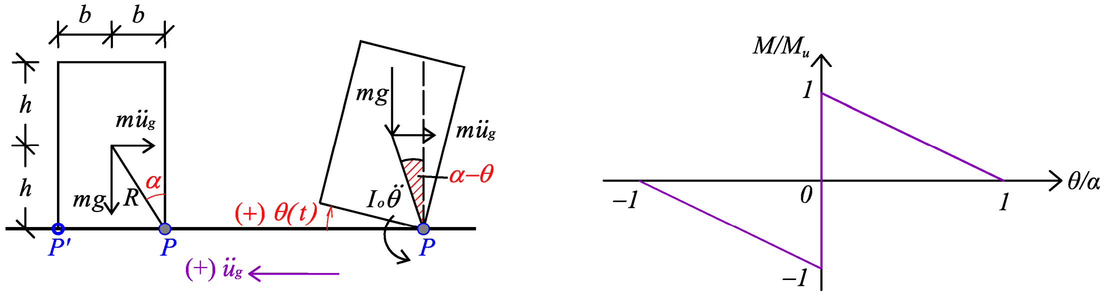

Figure 1. Rocking block on a rigid base and linearised resisting moment-rotation backbone curve in Eq.(2)

The non-linear equation governing rocking response of a rigid block is (Housner 1963)

$$I_o\ddot{\theta} + mgR\,\sin[\alpha - \theta\,\mathrm{sgn}(\theta)]\mathrm{sgn}(\theta) = +m\ddot{u}_g R\cos[\alpha - \theta\,\mathrm{sgn}(\theta)] \quad (1)$$

where I_o is the moment of inertia of the block with respect to its corner P or P' (for rectangular geometry, $I_o = 4mR^2/3$) and $sgn(\cdot)$ denotes the signum function. The positive sign on the right-hand side of the equations is to ensure positive rocking response for positive ground acceleration, as evident from the reference system of Fig.1a.

For slender blocks angle α is small; the above equation can be linearized using the first-order approximations $\sin(\alpha \pm \theta) \cong \alpha \pm \theta$, $\cos(\alpha \pm \theta) \cong 1$ and re-written in the form:

$$\ddot{\theta} - p^2\theta = +p^2\ddot{u}_g / g - p^2\alpha\,\mathrm{sgn}(\theta) \quad (2)$$

$p = (3g/4R)^{1/2}$ is a measure of the dynamic characteristics of the block. Since the restoring force is exclusively due to gravity (as in the classical pendulum problem), the intrinsic frequency p is independent of the block mass.

Assuming that sliding does not take place, initiation of rocking requires overcoming of the restoring moment due to self-weight, by the overturning moment due to inertia i.e., $m\cdot\ddot{u}_g h \geq m\cdot g\cdot b$. For slender blocks ($\alpha$<20 degrees) this can be written as $\ddot{u}_g/g \geq \alpha$. The ratio of slenderness over dimensionless peak pulse acceleration ($\alpha\, g/A_g$), to be referred hereafter to as *uplift strength* η, can be used as discriminant: if $\eta > 1$ no rocking occurs, if $\eta < 1$ rocking initiates at $t = t_{up}$, when $\ddot{u}_g(t_{up}) = \alpha\, g$.

In light of Fig.1, up to the point of impact the block rocks around the right edge (pivot point P) with positive uplift angles. After impact rocking continues around the left edge (pivot point P') with negative uplift angles. The transition from one pivot point to the other is accompanied by energy loss during impact, even for a block made of a non-dissipative material and an elastic base. The reduction in kinetic energy during transition is $r = (\dot{\theta}_i^+ / \dot{\theta}_i^-)^2$, subscript i standing for "impact". Assuming perfectly plastic impact (i.e., no bouncing) and using conservation of angular momentum, Housner (1963) evaluated r for slender rectangular blocks $\varepsilon = \sqrt{r} = 1 - 3/2\alpha^2$, which defines the familiar coefficient of restitution. Clearly this is an upper-bound estimate, as the true coefficient of restitution is always smaller than the one disregarding bouncing.

As far as the seismic excitation is concerned, the FEMA P695 (FEMA 2009) far-field ground motion set was selected, comprising 22 pairs of strong acceleration time histories without any directivity or soft-soil characteristics.

Numerical simulations

For performing the numerical analyses, we followed the original proposal by Prieto et al. (2004). Thus, a compact formulation was derived to incorporate nonlinearities stemming from: (a) the transition from one rotation pivot point to the other; (b) the energy dissipation during impact and the associated discontinuity in angular velocity; and (c) the geometric nonlinearities expressed by the trigonometric terms in Eq.(1). The equation can be written in dimensionless form as

$$\ddot{x} - f^2 x + f^2 \operatorname{sgn}(x) = \frac{f^2}{\eta}\ddot{\psi}(\tau) + \ln(\varepsilon)\,\dot{x}^2\delta(x)\,\operatorname{sgn}(\dot{x}) \tag{3}$$

where $x = \theta/\alpha$ denotes the normalised rocking angle, $\ddot{\psi}(\tau) = \ddot{u}_g(\tau)/A_g$ the acceleration-normalised earthquake waveform, $f = p\,t_d$, and $\tau = t/t_d$ dimensionless time. It is evident from the above expression that the problem parameters have been reduced to three: ε, f and η. As for the suite of far-field motions at hand a unique predominant period t_d is hard to identify, the effect of record frequency content has been ignored and p is used in the ensuing as a parameter indicative of block size. This is tantamount to using t_d=1s in Eq.(3).

Probabilistic approach

For the suite of 44 earthquake motions, the response was evaluated considering ten values of the restitution coefficient ε in the range (0.5-0.95), and twelve block radii (~0.07–70m) corresponding to characteristic frequencies p in the range (0.33–10s^{-1}) that is, 120 parameter combinations per record. Applying the methodology of incremental dynamic analysis and selecting peak ground acceleration as the intensity measure IM and peak rocking angle as the engineering demand parameter EDP, each record was scaled to cover the entire range of rocking response, from uplift, to rocking, to overturning. The peak rocking angles were evaluated for each motion that, in turn, was scaled by gradually increasing its acceleration amplitude so that overturning was encountered under all seismic records. To ensure the desired accuracy, 100 to 300 increments for each case were required depending on system characteristics. Considering an average of 200 increments per record, the total number of analyses exceeds 1 million (120x200x44).

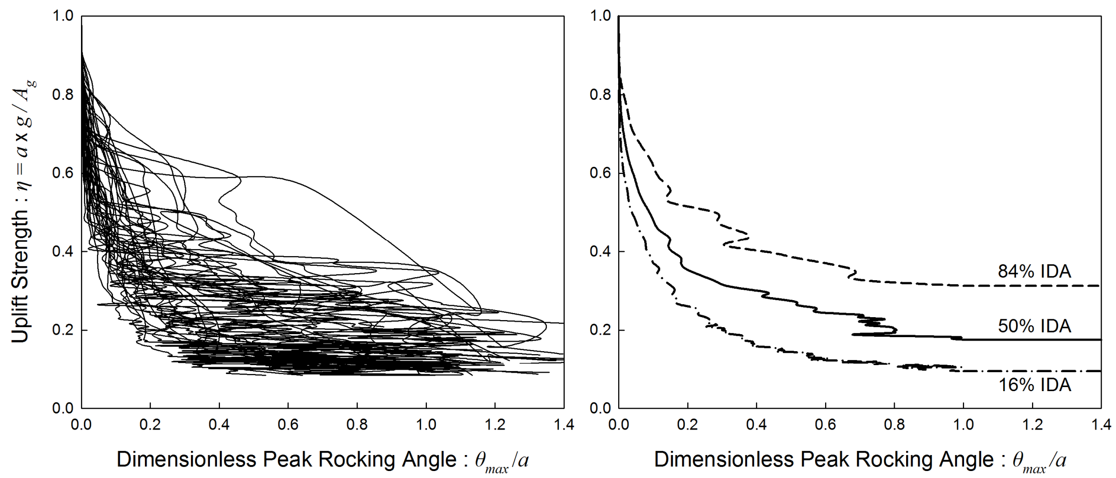

Figure 2. All forty-four IDA curves and their summary into their 16%, 50% and 84% fractiles for a given characteristic frequency p=2s^{-1} and coefficient of restitution ε=0.70

An example of the resulting IDA curve's for the whole suite of records and a given pair of ε, p, is provided in Fig.2a. The results are presented in dimensionless form, normalised by the block slenderness angle α. The IM is thus represented by uplift strength η and the EDP by the ratio (θ_{max}/α). The horizontal flatlines reached by each curve for large levels of intensity indicate that overturning has occurred and thus provide critical levels of intensity (and strength) capacity: IM_c or η_c. Given that rocking is a problem of instability, attempting to determine a critical value of response, EDP_c becomes an ill-posed condition of lesser significance. In fact, any sufficiently large value of response practically corresponds to the same level of IM_c. Thus, mainly for reasons of visualization, the static overturning criterion $(\theta_{max}/\alpha)_c=1$ is selected as an acceptable EDP_c. It could be similarly set to be “infinite” without any appreciable effect on the results. Wherever multiple flatilines appear, termed “structural resurrection” by Vamvatsikos and Cornell (2002), IM_c is taken equal to the uplift strength that corresponds to the lowest such flatline, or equivalently, the first occurrence of overturning. IDA results are finally summarized to provide the distribution of EDP given. This is achieved by calculating the 16%, 50%, and 84% fractile values of EDP for given IM levels. The 50% value (i.e., the median) is indicative of the central tendency, while the 16/84% percentiles represent the dispersion, as illustrated in Fig.2b.

The effect of block size, measured through the characteristic frequency p, is shown in Fig.3, where the 50% IDA’s are plotted for a given value of the coefficient of restitution. The safety wall separates the systems that overturn from the ones that do not. As evident from the graphs, the larger the value of the characteristic frequency (or, equivalently, the smaller the size of the block), the easier it is for overturning to occur. Conversely, the larger the size of the block the higher the ground motion intensity required to topple the block. This is in agreement with the findings of the analytical investigations based on the idealised waveforms and further investigations on near-source pulsive earthquakes.

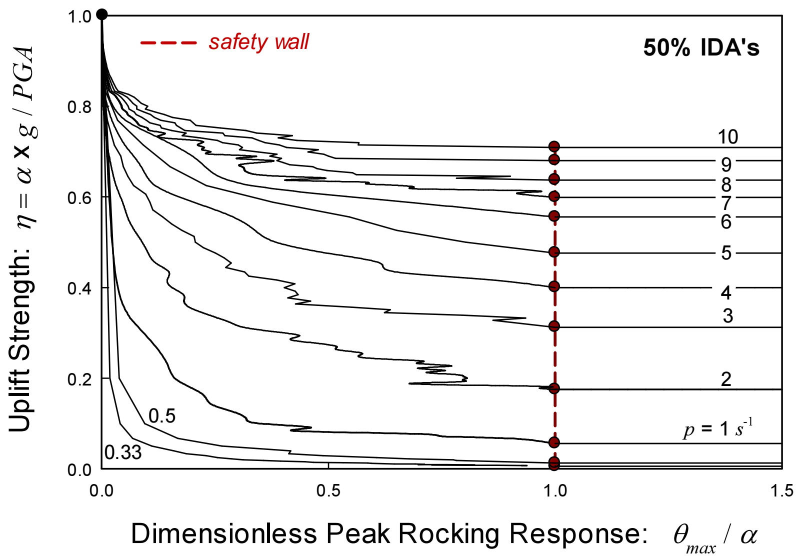

Figure 3. Median IDAs for different values of the characteristic frequency p; ε = 0.70

When summarising the IDA curves, one may use stripes of EDP given levels of IM (“horizontal statistics” with respect to Fig.2, thanks to the late Prof. H. Krawinkler), or stripes of IM given EDP (“vertical statistics”, similarly). The issue whether one should summarise given IM or EDP has been extensively discussed in Vamvatsikos & Cornell (2004) and it has been shown that they are essentially equivalent representations when a sufficiently large number of ground motion records is employed. For the case at hand, a comparison of the two alternative approaches has shown that 44 records are enough to remove any such issues. Nevertheless, it is always conceptually simpler to determine IM_c as the critical uplift strength η_c for a given $(\theta_{max}/\alpha)_c$ that is indicative of collapse (i.e., “infinite”), a value set to be 1.0 in our case. The ensemble of resulting values of overturning capacity thus estimated in terms of the percentile curves are grouped in Fig.4.

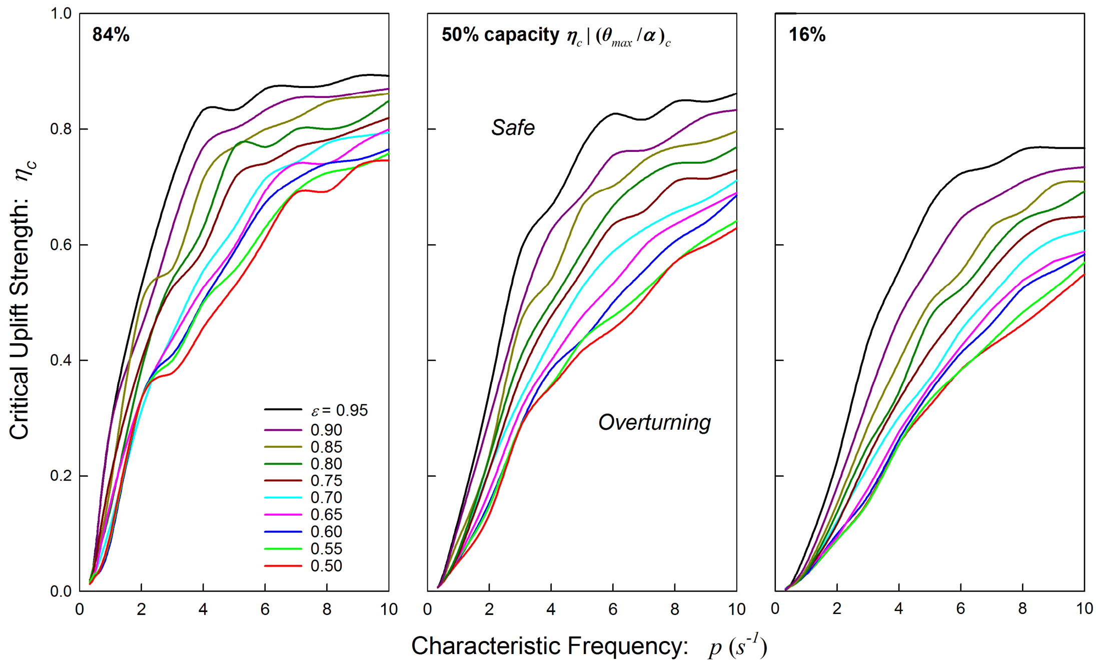

Figure 4. 16%, median and 84% capacity curves for the investigated systems

Given that we are only evaluating three point estimates of the η_c distribution, i.e. the 16/50/84% values, it is important to establish an appropriate distribution model for the entire population. The lognormal assumption has been typically employed for the collapse capacity of yielding systems and it may also be appropriate for the distribution of overturning capacity. To this end, the Lilliefors test (Lilliefors 1967) was employed to test the (null) hypothesis that log(η_c) values come from a normally distributed population. The majority of the tests (about 80%) show that we do not have enough evidence to reject this hypothesis at the 95% confidence level. The test p-values were generally higher than 10%. Thus, it may be stated in general that a lognormal distribution is an adequate model. Fig.5, provides two examples (out of 120 cases) of these distributions. Fig.5a is a typical example of cases with high p-values (p_{val}>20%) and shows good agreement with the lognormal distribution assumption. Fig.5b refers to the non-conforming cases of very low p-values (p_{val}<1%) where a right skew is apparent in the distribution. Better precision by means of additional increments in the area of calculated values of η_c seems to fix the problem.

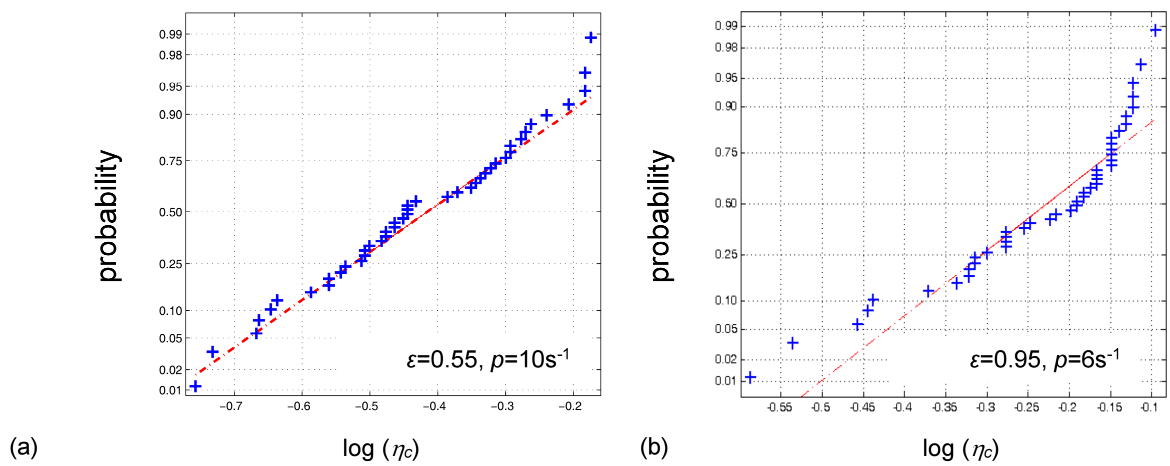

Figure 5. Lognormal probability plots of the overturning collapse capacity η_c
(a) p_{val}=55%; (b) p_{val}=0.3%

Overturning Criterion
A simple expression that describes a general overturning criterion, as function of the problem parameters η, p, ε is desirable. To this end, the produced capacity curves were approximated by means of nonlinear regression. The existence of the analytical solutions made this task particularly easy as the regressions were based on the rigorous criterion for overturning under a full-cycle rectangular pulse (Voyagaki et al 2014). With that starting point we assumed that the critical uplift strength for the suite of motions at hand can be cast in the form

$$\eta_c = a(1-e^{-bp})^c \tag{4}$$

where a, b, c are parameters depending on the coefficient of restitution ε. To achieve an estimate of η_c for different values of ε and p, a two-step regression was employed. First, coefficients a, b, c were fit via Eq.(4) for each given value of ε and each of the three different percentiles of η_c. Thus, for each percentile of η_c, three sets of a, b, c points versus ε were derived and subsequently fit by regression. For the median capacity these are described by the following first- and second-order polynomials plotted in Fig.6

$$a_{50} = 0.44 + 0.43\varepsilon \qquad b_{50} = 0.56 - 1.14\varepsilon + 1.25\varepsilon^2 \qquad c_{50} = 1.66 - 0.38\varepsilon + 1.4\varepsilon^2 \tag{5}$$

For dimensional conformity, p (measured in s^{-1}) in Eq.(4) should be multiplied by t_d=1s. Corresponding expressions were also produced for the 16% and 84% capacities:

$$a_{16} = 0.5 + 0.33\varepsilon \qquad b_{16} = 1.64 - 4.39\varepsilon + 3.44\varepsilon^2 \qquad c_{16} = 7.17 - 15.65\varepsilon + 12\varepsilon^2 \tag{6}$$

and

$$a_{84} = 0.64 + 0.24\varepsilon \qquad b_{84} = -0.66 + 2.32\varepsilon - 0.94\varepsilon^2 \qquad c_{84} = -2.28 + 10.3\varepsilon - 6.27\varepsilon^2 \tag{7}$$

The approximate capacity curves represented by Eqs (4) – (7) are shown in Figs 6 and 7. As evident in Fig.7b, the 16% capacity curves are not perfect at the lower values of ε, still, these are considered rather difficult to encounter. Further analyses will improve upon that case.

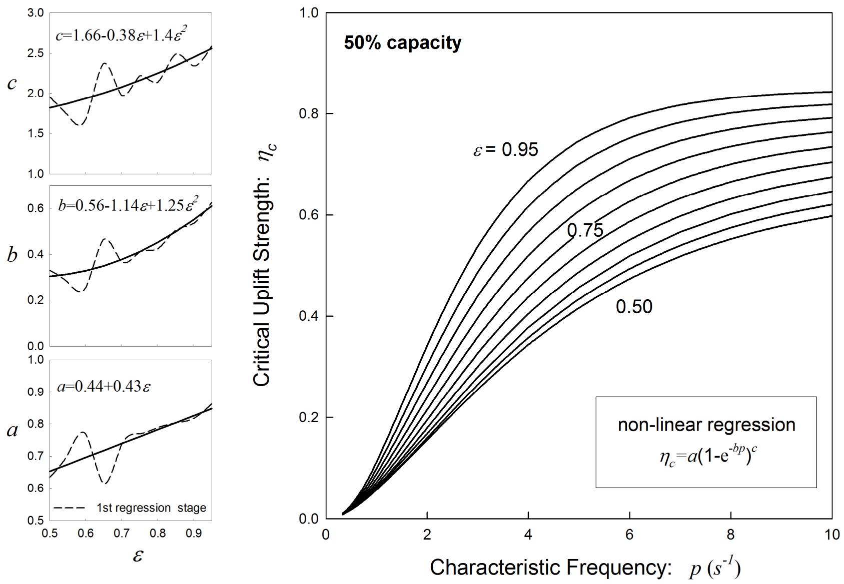

Figure 6. Median percentiles of critical uplift strength, calculated via nonlinear regression of the numerical data. The figures on the left represent the secondary fitting of the coefficients of Eq.(5) for different values of the coefficient of restitution

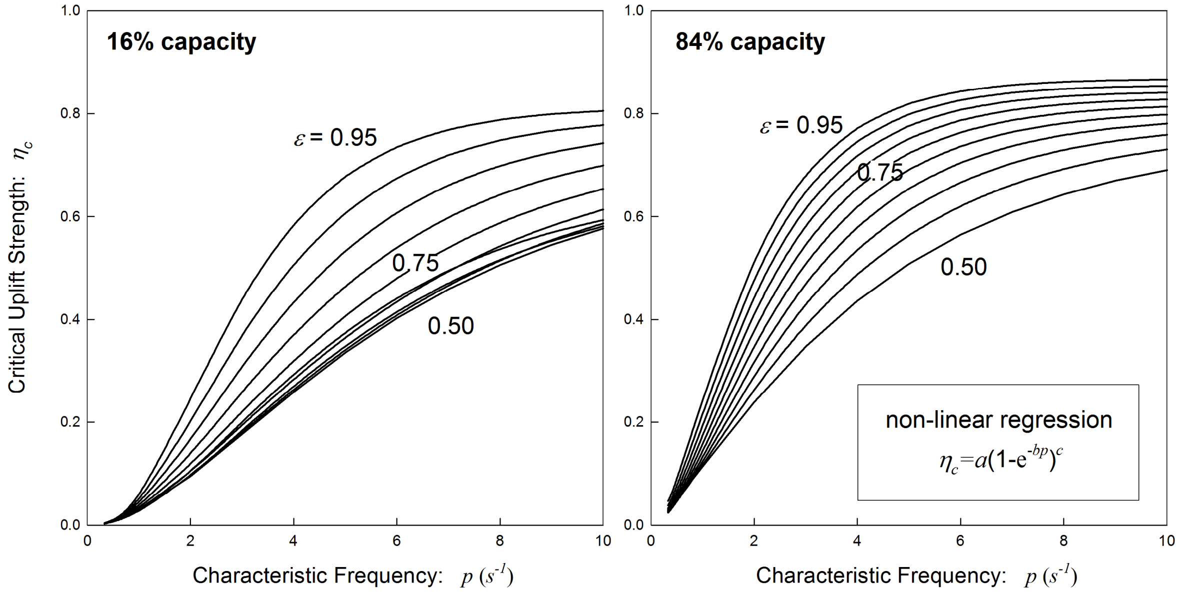

Figure 7. 16% and 84% percentiles of critical uplift strength, calculated via nonlinear regression of the numerical data; a, b, c from Eqs (6) & (7)

Peak rocking response

The maximum rocking angles may also be approximated via nonlinear regression, as shown in the ensuing. The parameters that need to be fitted are now increased by one (θ_{max}/α) and so are the regression stages involved in the analyses. One possible approach is maintaining fixed boundaries of the solution at $(\theta_{max}/\alpha\ ,\ \eta) = (0,1)$ and $(1,\ \eta_c)$, where the critical uplift strength is given by Eqs (4)-(7). The peak rocking response may thus be written as

$$\eta = \eta_c^{\frac{(1+m)\theta_{\max}/\alpha}{m+\theta_{\max}/\alpha}} \tag{8}$$

m being a parameter depending on block geometry p, and by means of the parameters A, B, C, on the coefficient of restitution ε. For the median, 16% and 84% capacities the following simple exponential formulae were produced.

$$m = Ce^{-\left(\frac{\ln p - A}{B}\right)^2} \tag{9}$$

$$A_{50} = 8.6e^{-3.6\varepsilon} \quad B_{50} = 8.1e^{-2.5\varepsilon} \quad C_{50} = 0.014e^{3.2\varepsilon} \tag{10}$$

$$A_{16} = 1.9e^{-1.4\varepsilon} \quad B_{16} = 2.7e^{-1.3\varepsilon} \quad C_{16} = 0.046e^{1.4\varepsilon} \tag{11}$$

$$A_{84} = 78e^{-8\varepsilon} \quad B_{84} = 3.9e^{-1.7\varepsilon} \quad C_{84} = 0.007e^{4.7\varepsilon} \tag{12}$$

A summary of the above equations is given in Fig (8) for the 50% values. Their applicability is presently limited to values of $\theta_{max}/\alpha > 0.15$. A comparison of the numerical data with the fitted curves described by Eqs. (8)–(12) is shown in Fig 9 where the fitted formula appears to generally underestimate the response, mainly due to the inflexibility of the fitted equation. The visualisation of the fitted formula is better achieved via the 3D plots in Fig 10 where all the problem parameters are present. It can be seen that the solution requires better fitting for small values of the rocking angle, a problem more apparent in the case of the 16% capacity curves.

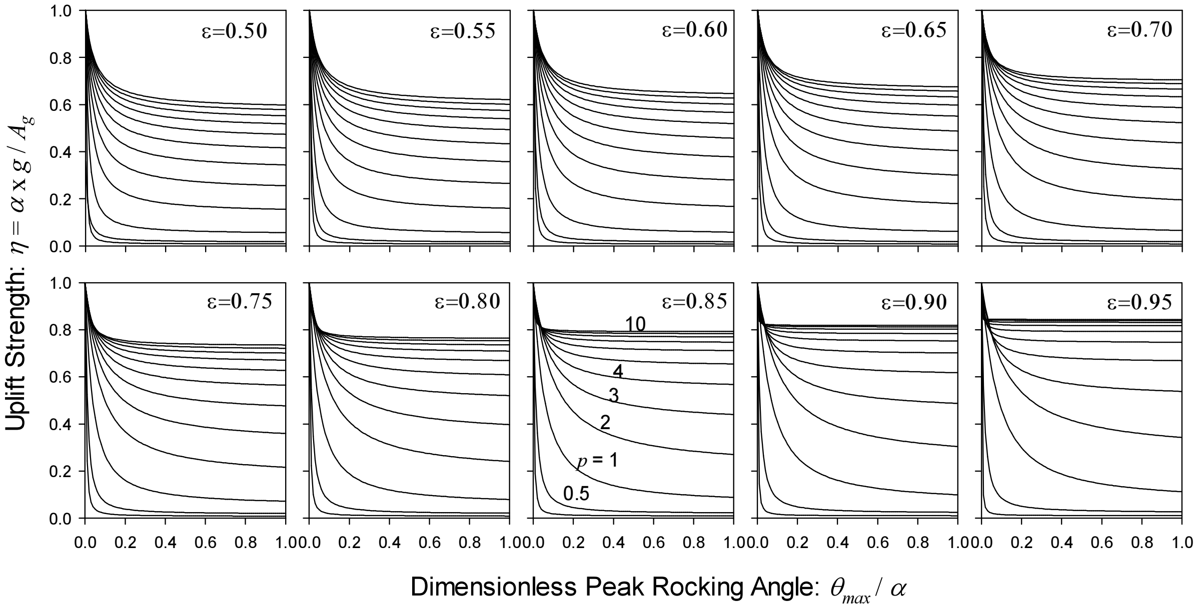

Figure 8. 50% quantiles of uplift strength as function of peak rocking response θ_{max}, normalised with slenderness angle α, calculated via nonlinear regression of the numerical data

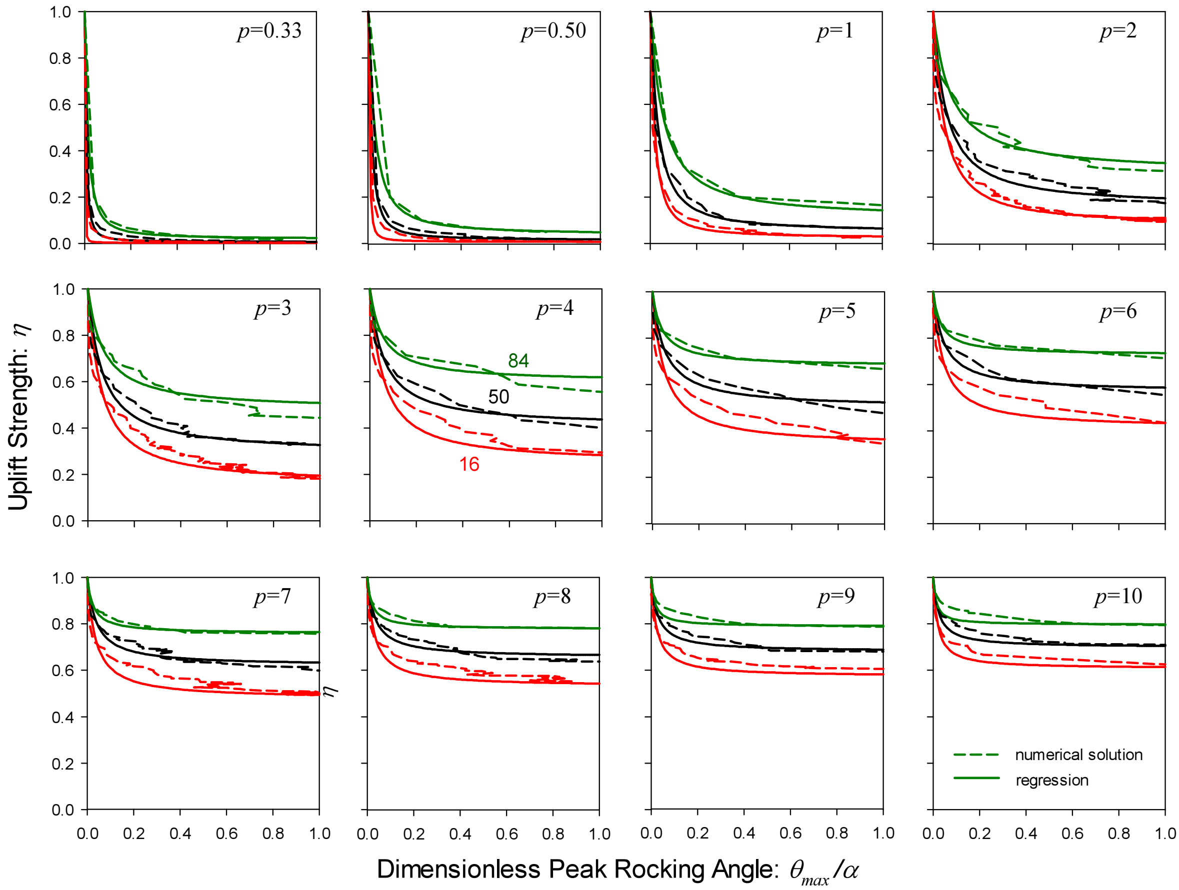

Figure 9. 16-50-84 percentiles of uplift strength as function of peak response. Comparison of numerical results with nonlinear regression. ε=0.7

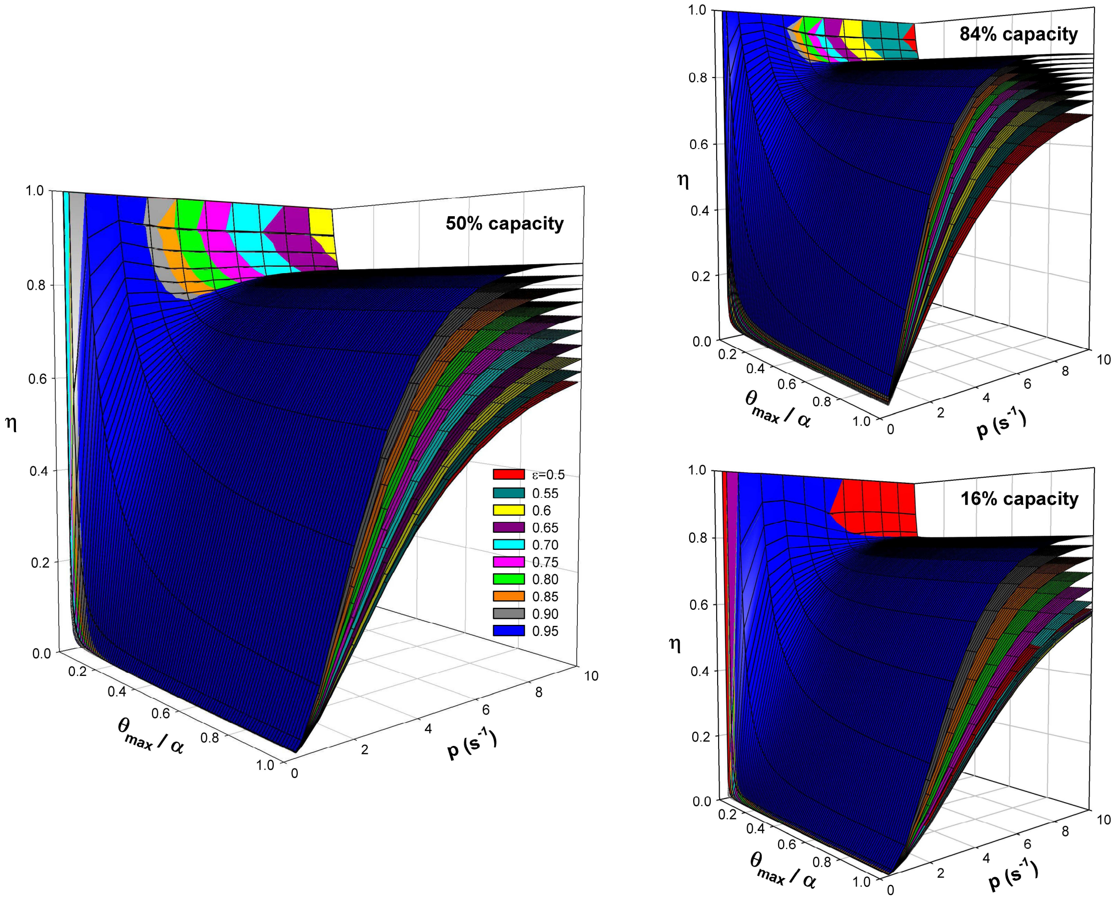

Figure 10. 16-50-84 percentiles of uplift strength η, calculated via nonlinear regression of the numerical data, as function of peak rocking response (normalised with slenderness angle α), characteristic frequency p and restitution coefficient ε

Conclusions

The rocking behaviour of a free-standing block resting on a rigid base and subject to 44 far-field earthquake motions was estimated numerically. Careful examination of the problem led to the following conclusions:

1. Overturning due to far-field seismic excitations may be reduced to three parameters: block size, expressed in terms of characteristic block frequency p, dimensionless uplift strength η (i.e., ratio of minimum required acceleration for initiation of uplift over peak ground acceleration) and coefficient of restitution ε.
2. The lognormal distribution is an adequate (although apparently imperfect) model for overturning capacity.
3. A simple expression based on closed-form solutions for the so-called safety wall can be exploited through non-linear regression techniques to provide a general probabilistic criterion for overturning under far-field ground motions.
4. The peak rocking response was approximated via simple fitted formulae that incorporate all the problem parameters.

The proposed expression allows for calculating both the median/mean and dispersion of response as a function of the coefficient of restitution and the characteristic frequency. The end result can be used to evaluate the probability of overturning for any rigid block resting on the ground, providing all the data needed for performance-based earthquake engineering applications.

Acknowledgements

Financial support was provided by Greece and the European Union (European Social Funds) through the Operational Program "Human Resources Development" of the National Strategic Framework (NSRF) 2007-2013, and by the European Research Executive Agency via Marie Curie grant PCIG09-GA-2011-293855.

REFERENCES

Dimitrakopoulos E and DeJong M (2012) Revisiting the rocking block: closed-form solutions and similarity laws, *Proceedings of the Royal Society*, 468(2144): 2294-2318

FEMA (2009) *Quantification of Seismic Performance Factors*, FEMA P-695 Report, prepared by the Applied Technology Council for the Federal Emergency Management Agency, Washington, DC

Housner GW (1963) The behavior of inverted pendulum structures during earthquakes, *Bulletin of the Seismological Society of America*, 52(2): 404-417

Lilliefors H (1967) On the Kolmogorov–Smirnov test for normality with mean and variance unknown, *Journal of the American Statistical Association*, 62: 399–402

Prieto F, Lourenço PB, Oliveira CS (2004) Impulsive Dirac-delta forces in the rocking motion, *Earthquake Engineering and Structural Dynamics*, 33(7): 839–857

Shi B, Anooshehpoor A, Zheng Y, Brune JN (1996) Rocking and overturning of precariously balanced rocks by earthquakes, *Bulletin of the Seismological Society of America*, 86(5): 1364-1371

Vamvatsikos D and Cornell CA (2002) Incremental Dynamic Analysis, *Earthquake Engineering and Structural Dynamics*, 31(3): 491-514

Vamvatsikos D and Cornell CA (2004) Applied Incremental Dynamic Analysis, *Earthquake Spectra*, 20(2): 523-553

Voyagaki E, Psycharis IN, Mylonakis G (2013) Rocking Response and Overturning Criteria for Free Standing Rigid Blocks to Single – Lobe Pulses, *Soil Dynamics & Earthquake Engineering*, 46: 85–95

Voyagaki E, Psycharis IN, Mylonakis G (2014) Complex Response of a Rocking Block to a Full-Cycle Pulse, *Journal of Engineering Mechanics ASCE*, 140(6), 04014024

Voyagaki E and Vamvatsikos D (2014) Probabilistic Characterization of Overturning Capacity for Simply-Supported Rigid Blocks, Proceedings of the 2nd European Conference on Earthquake Engineering and Seismology (2ECEES), Istanbul, Turkey